

Results and comparison of a cladding pumped fiber simulation using a decagon-shaped fiber

D. Young, C. Roychoudhuri

University of Connecticut, Storrs, CT 06269 USA
david.young@uconn.edu, chandra@phys.uconn.edu

Abstract: This paper presents a simulation technique developed to concurrently model the pump and laser power evolution in a cladding pumped rare-earth doped fiber. The simulation technique uses a series of scaling factors to dramatically decrease simulation run-times, while maintaining accuracy. This approach differs from previous methods in that it can simulate arbitrary pump cladding shapes. The results of the simulation are validated using a decagon-shaped cladding pumped, ytterbium doped fiber. Good correlation is found between the simulated and experimental pump evolution and conversion efficiency.

© 2003 Optical Society of America

OCIS codes: (060.2280) Fiber design, (140.3510) Lasers, Fibers

References and Links

1. E. Snitzer, H. Po, F. Hakimi, R. Tumminelli, B.C. McCollum, "Double-clad offset core Nd fiber laser," in *Proc. Of Optical Fiber Sensors '88*, pp. PD5, (1988).
2. A. White, S. Grubb, *Optical Fiber Telecommunications IIIB*, (Academic Press, 1997), Chap. 7.
3. H. Po, E. Snitzer, R. Tumminelli, L. Zenteno, F. Hakimi, N.M. Cho, T. Haw, "Double-clad high brightness Nd fiber laser pumped by GaAlAs phased array," in *Optical Fiber Communication Conference* (Optical Society of America, Washington, D.C., 1989). Pp. PD7
4. M. Muendel, "Optical fiber structure for efficient use of pump power," US Patent # 5,533,563, 1996.
5. D. DiGiovanni, "Method of making a cladding pumped fiber structure," US Patent # 5,873,923, 1999.
6. M. Muendel, "Optimal inner cladding shapes for double-clad fiber lasers," in *Conference on Lasers and Electro-Optics, Technical Digest*, (Optical Society of America, Washington DC, 1996), pp. 209.
7. L. Qiao, J. Wang, "A modified ray-optic method for arbitrary dielectric waveguides," *IEEE J. Quantum Electron.*, **28**, 2721-2727, (1992).
8. M. Feit, J. Fleck, "Light propagation in graded index optical fibers" *Appl. Opt.*, **17**, 3990-3998, (1978).
9. D. Kouznetsov, J. Moloney, "Efficiency of pump absorption in double-clad fiber amplifiers. II. Broken circular symmetry," *J. Opt. Soc. Am. B.*, **19**, 1259-1263, (2002).
10. D. Kouznetsov, J. Moloney, "Efficiency of pump absorption in double-clad fiber amplifiers. III. Calculation of modes," *J. Opt. Soc. Am. B.*, **19**, 1304-1309, (2002).
11. L. Thylen, E. Wright, G. Stegeman, C. Seaton, J. Moloney, "Beam propagation method analysis of a nonlinear directional coupler," *Optics Lett.*, **11**, 739-741, (1986).
12. A. Liu, K. Ueda, "The absorption characteristics of circular, offset, and rectangular double-clad fibers," *Optics Comm.*, **132**, 511-518, (1996).
13. B. Kerrinckx, P. Even, D. Pureur, "New theoretical model of ytterbium-doped double-clad fiber for laser application," in *Optical Fiber Communication Conference* (Optical Society of America, Washington, D.C., 2001). Pp. TuI3-1.
14. A. Siegman, *Lasers*. (University Science Books, 1986), Chap. 3, 7.
15. H. Pask, J. Archambault, D. Hanna, L. Reekie, P.St.J. Russell, J. Townsend, A. Tropper, "Operation of cladding pumped Yb³⁺-doped silica fibre lasers in the 1 μ m region," *Electron. Lett.*, **30**, 863-864, (1994).

1. Introduction

In 1988, a solution was found for the problem of producing fiber lasers and amplifiers that produce output powers in the >1 W range. Instead of concentrating on coupling pump energy only into the rare-earth doped single-mode core of the fiber, a cladding pumped configuration

was used [1]. This approach allowed coupling of a high power multi-mode pump source, such as a laser diode array, into the first clad which has a diameter $>100\mu\text{m}$, a factor of 10 or greater larger in diameter than the single-mode core. In cylindrical clad optical fiber, only the HE_{1m} [2] modes have energy at the center of the waveguide, once the rare-earth doped core absorbs this energy, only outer skew modes will exist. These skew modes can be perturbed by unintended index variations, stresses, and core-clad interface defects which scatter or refract the skew modes, increasing the probability of interaction with the core. Such perturbations can also cause leakage of the single-mode laser light, given the rare-earth doped core typically has a weaker guiding condition than the pump clad. With modern fiber manufacturing processes, most undesirable fiber defects such as point defects, unintended index variations, etc., that could scatter higher order mode energy towards the rare-earth doped core are avoided, creating the need for a intentional, controllable scattering mechanism. Solutions to this problem included rectangular shaped pump clads [3], hexagons [4] and concave polygons [5]. The last two shapes help to maximize the useful surface area being pumped, ease coupling to standard fibers, and simplify the fiber manufacturing process.

Propagation modeling of double-clad fibers can be done using ray trace techniques [7], which are effective for modeling the propagation in the clad where the physical dimensions are substantially larger than the wavelength of light being propagated. Ray trace techniques are not well suited for calculating propagation in the single-mode core of a cladding pumped fiber, instead, single-mode propagation is often handled by beam propagation methods (BPM) [8]. BPM techniques, which are generally used for modeling diffractive/refractive phenomenon, can be expanded to handle non-linear events via the split-step Fourier transform (SSFT) technique [9] which treats the propagation of the beam and the nonlinearity in the propagation material as two or more discrete steps. The use of the SSFT in fiber models has largely focused on understanding the influence of nonlinear index variations in the core of single mode fibers during transmission. Other methods utilizing approximate images [10] and using perturbation theory by use of an analogy with quantum mechanics [11] have been explored.

This paper will describe an SSFT model developed for simulating cladding pumped rare-earth doped fibers. This technique simultaneously models the pump propagation in the multimode shaped clad, and the pump absorption and lasing buildup in the rare earth doped single-mode core. The developed model describes the intensity and phase profiles of the multimode pump energy in arbitrary shaped pump claddings. This is unique compared to previous models developed for analytically tractable shapes [12, 13]. An overview of the model development will be followed by simulation results for a decagon-shaped double-clad ytterbium doped fiber. The results from the model will then be compared against the measured performance of a cladding pumped fiber with a novel decagon-shaped pump clad.

2. Model Development

In order to model the propagation and laser dynamics in the cladding-pumped rare-earth doped fiber, Maxwell's equation, as shown in Eq. (1) is solved numerically.

$$\frac{\partial \vec{E}}{\partial z} = -j \frac{1}{2k} \nabla_{\perp}^2 \vec{E} - j \frac{\mu_0 \omega^2}{2k} \vec{P} \quad (1)$$

Our model uses SSFT methods for propagation in the arbitrarily shaped cladding region as well as the core. This consists of reducing the square of the gradient of the electric field component of Eq. (1) to the vector components perpendicular to the direction of propagation through the Fresnel approximation, then propagating a sampled version of the wave front through a series of small steps via two-dimensional Fourier transforms. This model, as developed, concurrently solves the second-half of Eq. (1) to obtain the material dynamics.

This is done through the polarization of the material, and it's relationship to the electric field via:

$$\bar{P} = \mathbf{e}_0 \mathbf{c}_{at} \bar{E} \quad (2)$$

Where $\bar{\mathbf{c}}_{at}$ is given by [14]:

$$\bar{\mathbf{c}}_{at}(\mathbf{w}) = \frac{-j}{4\mathbf{p}^2} \frac{I^3 \mathbf{g}_{rad,2 \rightarrow 1}}{\Delta \mathbf{w}_a} \left(\frac{g_2}{g_1} N_1 - N_2 \right) \frac{1}{1 + 2j(\mathbf{w} - \mathbf{w}_a) / \Delta \mathbf{w}_a} \quad (3)$$

Where $\gamma_{rad,2 \rightarrow 1}$ is the radiative decay rate from the upper to the lower lasing levels, $\Delta \omega_a$ is the atomic linewidth, ω_a is the material resonance frequency, and g_1 and g_2 are the levels of degeneracy for the lower and upper lasing state energy levels. N_1 and N_2 , the populations of the lower and upper levels of the lasing transition, are a function of the energy density of the pump in the rare-earth doped core, as well as the laser energy evolution of the length of the fiber. The susceptibility can be separated into atomic phase shift and amplitude components through $\chi_{at} = \chi' + j\chi''$, χ'' is responsible for either loss or gain in the material. The mid-band value of the susceptibility is given by [14]:

$$\mathbf{c}'' = \frac{1}{4\mathbf{p}^2} \frac{I^3 \mathbf{g}_{rad,2 \rightarrow 1}}{\Delta \mathbf{w}_a} \left(\frac{g_2}{g_1} N_1 - N_2 \right) \quad (4)$$

The values for N_1 and N_2 as a function of length along the fiber are calculated at each sampled point using solutions to the laser rate equations, which include the signal intensity in the rare-earth doped core and the pump intensity in the core. The rate equations used in this model are for a three-level lasing system, this allows the behavior of ytterbium, which in silica exhibits both quasi-three level behavior dependant on the lasing transition, to be modeled. The propagation and material dynamics are calculated in a stepwise manner that assumes that the propagation and material dynamics can be treated separately given small (sub-wavelength) step sizes. Two elements must be considered, the change in amplitude distribution and phase as a function of propagation, and the change in amplitude as a function of absorption (pump energy) or emission (core energy). The propagation technique used assumed that the paraxial condition holds – which is the case for the fiber modeled. The Fresnel approximation, which simplifies the description of the field, and the slowly varying envelope approximation are used to reduce the propagation equation to:

$$\bar{u}(x, y, z) = \frac{j}{(z - z_0)I} \iint \bar{u}(x_0, y_0, z_0) e^{\frac{-jk(x-x_0)^2 + (y-y_0)^2}{2(z-z_0)}} dx_0 dy_0 \quad (5)$$

Where x_0 , y_0 , and z_0 are the initial coordinate of the array point being propagated, and x , y , and z is the array point coordinate post-propagation – this reduced form is related to the electric field through $E(x,y,z) = u(x,y,z) \exp(-jkz)$. This equation has the form of a convolution between the complex field and the exponential term [14], thus propagation is done by Fourier transforming the initial field and the exponential term, multiplying them, then inverse Fourier transforming to get the propagated field description. If the array spacing and propagation distance are invariant, then the exponential term need only be Fourier transformed once, then saved, reducing the simulation time.

The material kinetics, which are described by the second part of Eq. (1), are simulated in part by calculating the difference in the upper and lower lasing states – as the model is for a three level system, it is assumed that the decay rate from the upper pump energy level to the upper lasing energy level is fast, thus the population of this state can be ignored. The pump rate, R_{13} , for each array point must be calculated – the pump rate for any given array point is given by $\sigma_p I_p / h\nu_p$, where σ_p is the pump absorption cross section in the core, I_p is the pump

intensity at any array point, and ν_p is the frequency of the pump light. For the “signal” in the rare-earth doped core, the emission cross section probability, W_e , is given by $S_e I_s / h\nu_s$, and the absorption cross section probability, W_a , is given by $S_a I_s / h\nu_s$, where the $\sigma_{a,e}$ is the signal absorption/emission cross section in the core, I_s is the signal intensity at any array point, and ν_s is the frequency of the signal light. The measured material properties were used in the model. The value used for σ_p was $1.5 \times 10^{-21} \text{ cm}^2$, $\sigma_e = 1.3 \times 10^{-20} \text{ cm}^2$, and $\sigma_a = 5.8 \times 10^{-21} \text{ cm}^2$. Given these terms, the population difference, ΔN , for a degenerate transition is given by:

$$\Delta N = \left[\frac{N_0}{W_a + W_e + \frac{1}{t_2} + R_{13}} \right] \left[\frac{g_2}{g_1} \left(W_e + \frac{1}{t_2} \right) - (W_a + R_{13}) \right] \quad (6)$$

The degeneracy levels for ytterbium in silica are $g_1=4$, $g_2=3$. N_0 is the ion density in the doped core, which was set at $4.4 \times 10^{19} \text{ cm}^{-3}$. From [14], χ'' at mid-band is given by $\chi'' = \Delta N \sigma_e \lambda / 2\pi$, where σ_e is given by $(1/2\pi)(\gamma_{\text{rad}}/\Delta\omega_a)\lambda^2$. Stepping a small distance $\Delta z = z - z_0$, the change in the magnitude of the input electric field, E_{in} as a function of material dynamics can now be given by;

$$\Delta E = -j \frac{k \mathbf{c}''}{2n^2} E_{in} \Delta z \quad (7)$$

One problem with simulating with multiple optical waveguides concurrently is the different spatial frequency of the sampling points required by the different sizes of the waveguides. The spatial frequency used in modeling a double-clad fiber is driven by the requirement to model the single-mode core accurately. In this model, the core and the cladding wave front arrays are of equal spatial frequency – this was done to ensure that the calculation of the pump energy in the rare-earth doped core was accurate. This led to a very large number of sampled points to model both a core and cladding where the diameter ratio is 20:1, or greater. In order to limit the number of points used in the simulation wave front arrays, the size of both the pump clad and the core were scaled down proportionately. Using Eq. (4) [6], the overall small-signal cladding pumped fiber absorption α_{fiber} can be scaled by varying the small-signal core absorption α_{core} as well as the core and cladding area.

$$\mathbf{a}_{\text{fiber}} = \mathbf{a}_{\text{core}} \frac{A_{\text{core}}}{A_{\text{clad}}} \quad (8)$$

By reducing the cladding diameter, thus the area, while maintaining the $A_{\text{core}}/A_{\text{clad}}$ ratio, the size of the arrays being propagated can be decreased, reducing the overall simulation time. Reduction of the core and cladding diameter must be accompanied by a reduction of the pump and lasing wavelength in the model in order to preserve the modal behavior of the waveguides. The number of modes in the clad, thus the modal distribution is directly proportional to the ratio of the square of the clad radius and the wavelength of light being propagated. As the core radius decreases, the wavelength of light in the core must also be decreased in order to maintain the single-mode guiding condition. The model uses Fourier transform techniques for propagating the wave front – as the point density goes as 2^3 , it becomes important to carefully pick the array size – a 256×256 array requires 65,536 Fourier transforms per step, while the next density, 512×512 , requires 262,144 Fourier transforms. The fiber being modeled is nominally 230 microns in diameter, with an 8-micron diameter core. At the Nyquist limit, it would require over 4 million Fourier transforms per step to properly propagate the field in both the core and clad. Using the scaling of the core/clad ratio, combined with scaling of the core absorption coefficient allowed for much shorter simulation times. In the simulation results shown below, a device with scale lengths up to 80 meters in length was simulated in less than 12 hours of run time on a current Pentium class personal computer.

3. Model results

The physical parameters required for running the simulation were measured on a sample of the fiber being used to test the accuracy of the model. The measurement equipment used a multi-stripe laser diode with a nominal center wavelength of 918 nm. For the model, the core absorption coefficient at this wavelength was set to be 0.7 cm^{-1} . As was mentioned in Section 2, a scaling factor, based on Eq. (8) was used to scale the model results to the experimental fiber. For the simulation a cladding diameter (circle inscribed into the decagon) of $18.4 \mu\text{m}$ was used. The core diameter was reduced to $0.64 \mu\text{m}$ to maintain the same core to cladding area ratio. In order to maintain the same capture area of the core, the pump and lasing wavelengths were scaled down to maintain the single-mode condition in the rare-earth doped core. The pump clad numerical aperture was set to 0.48. In the experimental measurements, the pump beam from a fiber coupled laser diode with a $600 \mu\text{m}$ 0.22 NA fiber was coupled into a $230 \mu\text{m}$ 0.48 NA fiber, which was run through a Newport mode scrambler to assure proper mode mixing. The output of this fiber was collimated, and then launched into the double-clad fiber using a 0.45 NA molded aspherical lens – the fiber was positioned until the laser power out was maximized. In the model a flattop beam that filled the aperture was used. In this model, the fiber shape is used to randomize the modes to increase the cladding pumped absorption per unit length – this randomization effect also acted to minimize any difference between simulation and model depending on fiber launch conditions. The core absorption rate in the model was also increased, once again to use the scaling described in Eq. (8). The total scaling factor for the core and cladding areas, and the core absorption rate was 500. Figure 1 shows the simulated evolution of the pump power and lasing power over the lengths modeled.

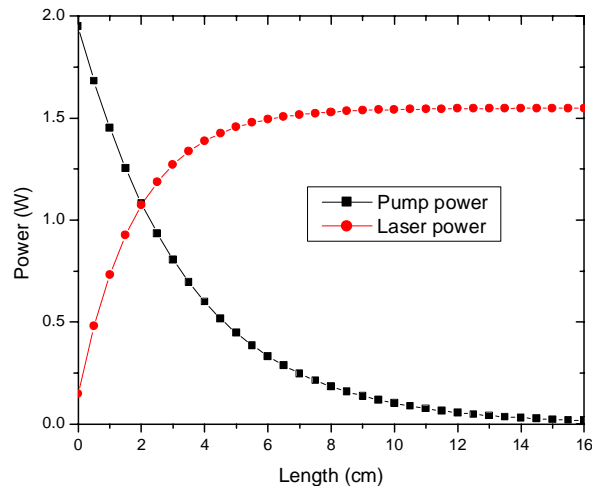


Fig. 1. Pump and laser (signal) power evolution as a function of length for the simulated decagon-shaped fiber. In this case a pump power of 2 watts was used. The simulation length was 16 cm.

4. Experimental fiber

The fiber that was developed for this work was a double clad, ytterbium doped fiber. The fiber was unique to fibers previously reported in the literature as its pump clad has a decagonal shape – an end micrograph of this fiber is shown in Fig. 2. The ytterbium was incorporated into the core using the solution-doping technique. The second clad was a UV-cured hard polymer, which against the pure silica pump clad yielded an NA of 0.48. The construction process for both the preform and fiber utilizes standard manufacturing techniques; the only major difference being a machining step to produce the shaped preform.

This shape is similar to standard round fibers, which simplifies fusion splicing and decreases pump loss at the splice. The decagon also has a larger surface area than other shaped fibers previously discussed in the literature – this allows for greater convective cooling in high power applications. The core absorption was 0.7 cm^{-1} – this was measured at 918 nm, the nominal pump wavelength of the measurement setup used.

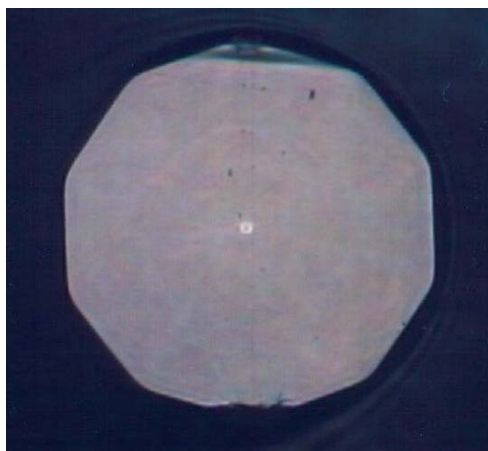


Fig. 2. End micrograph of the experimental decagon-shaped fiber. The diameter of the pump clad is nominally $230 \mu\text{m}$. Cleave damage obscures the upper and lower apices.

5. Comparison of simulation data to experimental data

Two metrics will be used to validate the simulation results to the experimental fiber – the pump power evolution as a function of device length, and the fiber conversion efficiency as a function of length. In the simulation, the laser cavity was defined by a high reflector at the lasing wavelength at the pump end, and the Fresnel reflection of the cleaved distal end of the fiber. In order to properly validate the model results, the experimental fiber was tested the same way. The pump power evolution data for the experimental fiber and the simulation are shown in Fig. 3. In this case an initial pump power of 2 watts was used for both the experimental and simulation data. Multiple experimental trials were done to understand the variation between multiple fiber lots. The peak cladding pump absorption from the model was 0.25 dB/m , the peak experimentally measured absorption was 0.23 dB/m . It was noted when making the comparison between the simulation and experimental results that the scaling technique used is sensitive to the scaling of the small signal absorption of the core. In heavily doped fibers the core attenuation coefficient is difficult to measure, as the cutback lengths needed to perform the measurements are fairly small (on the scale of centimeters) in order to detect signal at the pump wavelength. If the cutback length is not carefully measured, then the core absorption number will vary significantly. This variation, compounded with the multiplicative scaling of the core absorption described in Eq. (8), can lead to unacceptable offsets between simulated and experimental data. For this work, the core absorption of the experimental fiber was measured several times, and the mean value was fed back into the simulation in order to determine the accuracy of the simulation technique.

The range of lengths used in Fig. 3 represent typical device lengths for cladding-pumped fibers with pump clad diameters of this size range – shorter lengths result in excessive pump loss, longer lengths can lead to reabsorption of laser light in quasi three-level lasing systems like ytterbium in silica. The model data reflects the scaling factor discussed in Section 3. The correlation between the model and experimental data was quite good, with the model results showing a slightly higher absorption rate than the experimental data.

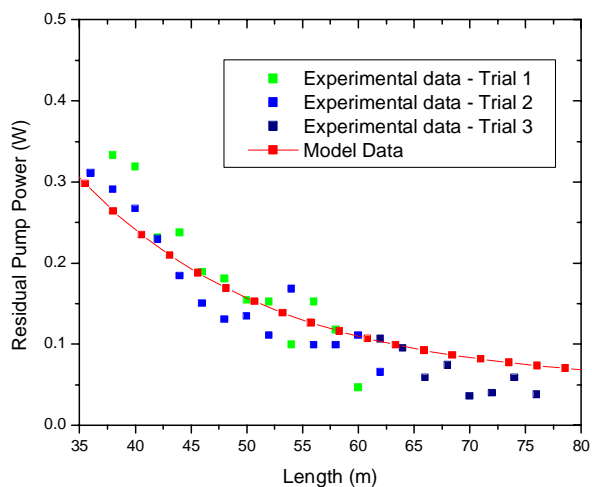


Fig. 3. Simulated and experimental pump absorption as a function of length for the 230 μm diameter decagonal fiber. The length scale chosen reflects a range of typical device lengths for cladding pumped devices.

The conversion efficiency (CE) of the fiber was also simulated and measured. The conversion efficiency is defined as the ratio of the laser output power and the absorbed pump power. The simulation calculated the build-up of the laser power as a function of length, and the absorbed pump power is simply the difference between the launched and the residual pump power. The comparison between the simulation and experiment is shown in Fig. 4.

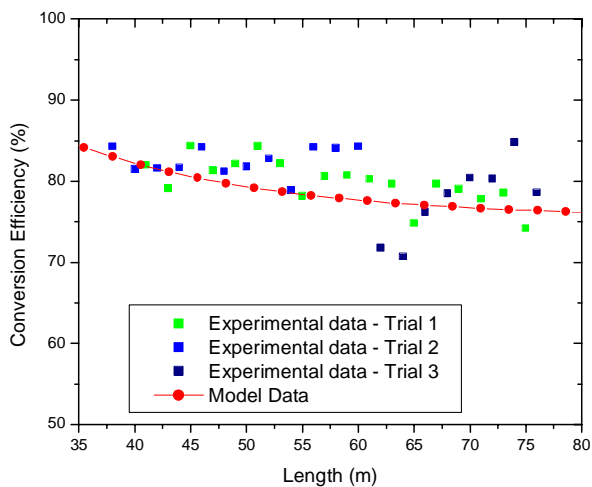


Fig. 4. Simulated and experimental conversion efficiency as a function of length for the 230 μm diameter decagonal fiber.

The correlation between the modeled CE and the experimental data was once again quite good. Note that the CE goes down as the length increases. As the CE goes as the ratio of the laser output power to the absorbed pump power, this indicates a re-absorption of the laser energy in the core at longer lengths – this action was shown in the model data, and confirmed by the experimental data. Note that the simulated conversion efficiency does not include any losses outside of re-absorption of the laser light generated in the core. The close correlation between the simulated and experimental data indicates that the experimental fiber had very low extrinsic loss.

The lasing wavelength in the experimental fiber, with no external control, varied between 1075 and 1080 nm over the lengths measured. Given a nominal pump wavelength of 920 nm, this yielded an average quantum efficiency of 93%, this indicates a very low degree of excess loss.

6. Conclusion

We have developed a modeling technique that can be used to simulate the propagation of multimode pump energy in the pump clad of a clad pumped fiber, as well as the propagation in the single-mode rare-earth doped core – the model concurrently simulates the lasing action in the rare-earth doped core. The method of scaling, described in Section 2, allows for realistic run-times when using SSFT techniques for modeling propagation in the pump clad and single mode core, while simulating the lasing build-up in the rare-earth doped core and the pump decay in the pump cladding. This results of the model discussed include the pump power evolution in the pump clad of the fiber and the laser power evolution in the ytterbium doped core. These results were compared against to a ytterbium doped cladding pumped fiber with a decagon shaped clad. Reasonable correlation exists between the model and experimental data. As was confirmed by both the model and experimental data, this fiber has a high absorption coefficient of 0.25 dB/m (modeled), and 0.23 dB/m (experimental) for a 230 μm diameter fiber pumped at 918 nm. The conversion efficiency, from both the model and experimental fiber, compared favorably with prior work in cladding pumped ytterbium-doped fiber lasers [15], typically over 80%. Additional work exploring the variation in the pump-clad size of the decagon-shaped fiber, as well as an octagonal shaped pump clad will be described in detail in a future paper. The experimental data from these fibers indicate that the high conversion efficiency shown in this sample fiber is likely a function of the fiber manufacturing process – initial measurements of the octagonal fiber also show conversion efficiencies exceeding 80%.

Acknowledgements

The authors would like to gratefully acknowledge OFS Optics, Avon, CT for the donation of the double-clad fiber used in this research.